Journal of Thermal Analysis and Calorimetry
https://doi.org/10.1007/s10973-024-13174-9

Optical observation and combustion properties during paper sludge fast heating

Qinzheng Teng[1,2] · Cen Sun[1,2] · Xiaolin Wei[1,2] · Sen Li[1,2]

Received: 11 August 2023 / Accepted: 4 April 2024

Abstract
The challenge of paper sludge disposal has become an important environmental issue; therefore, the combustion characteristics of paper sludge need to be examined. In this paper, the combustion of paper sludge particles under different atmospheres was analysed and investigated using a flat flame burner and optical observation techniques under fast temperature rise conditions. The combustion of paper sludge could be divided into a preheating stage, volatile combustion stage, and coke combustion stage. The changes in oxygen content had different effects on the different stages of combustion. The increase in oxygen content had no significant impact on the ignition time of the sludge particles; however, the flame brightness significantly increased. The CH* free radical appeared in the most intense stage of combustion and was depleted before the volatile flame disappeared. A higher oxygen content correlated to a faster CH* depletion. The influence of the oxygen content on the combustion rate and burnout degree of the sludge particles was investigated by comparing mass loss data and heating data. The maximum temperature and heating rate also increased with increasing oxygen content. The reduced oxygen concentration could not fully penetrate the ash layer on the surface of the particles and react with the interior sludge, resulting in a lesser degree of sludge particle burnout.

Keywords Combustion · Biomass fuel · CH* radical · Paper sludge · Optical observation · Fast heating

Introduction

The paper industry is important in national industry development of and social civilisation construction, and the level of production and consumption of paper can be regarded as the level of modernisation and civilisation of a country. China is a large paper-making country, and according to statistics, in 2020, China produced a total of 254.98 million tonnes of pulp, paper and paperboard and paper products together [1]. For every tonne of paper, 50 kg of dry sludge is created as byproduct [2]. As a result, a large amount of paper sludge is produced per year.

Paper sludge is usually considered a typical biomass fuel, which is mainly composed of lignin, cellulose and hemicellulose. It has a high organic component content (45–55%) and high ash content (approximately 45%) [3]. According to Saastamoinen et al. [4], paper sludge is a kind of biomass with a low calorific value, and it is difficult to ignite, more difficult to completely burn, and difficult to incinerate. Clearly, the combustion of paper sludge needs to be explored to achieve its efficient and clean treatment.

Some researchers have focussed on improving the combustion quality of paper sludge. To increase the flame stability and shorten ignition delay, the current technique dries or roasts the sludge to form a fuel pellet type shape [5]. Treated biomass has better combustion characteristics with a greater heat of reaction, and the activation energy of cellulose, an important component of biomass, is reduced after drying or roasting [6, 7]. However, more tedious pretreatment processes, such as crushing and baking, require the redesign and modification of the pulverised coal furnace and produces large amounts of fly ash, causing ash build-up, slagging and corrosion problems in the boiler. Wang et al. [8] explored the pyrolytic properties of paper sludge and applied the hydrothermal carbonation method to a pyrolysis experiment; specifically, the paper sludge was heated in an

✉ Xiaolin Wei
xlwei@imech.ac.cn

[1] State Key Laboratory of High-Temperature Gas Dynamics, Institute of Mechanics, Chinese Academy of Sciences, Beijing 100190, China

[2] School of Engineering Science, University of Chinese Academy of Sciences, Beijing 100049, China

Published online: 23 May 2024

aqueous solution at high pressure, and the average activation energy of pyrolysis was calculated.

Most studies have focussed on the combined combustion of sludge and other biomass or coal powder. Zhang et al. [9] analysed the sludge/coal blending characteristics, where sludge was blended with pulverised coal in a certain ratio for combustion, and the sludge and pulverised coal interacted at a specific temperature to promote combustion. Some studies are related to sewage sludge that can be used as a reference. Bi [10] investigated the effect of mixed combustion of sludge and coal powder in an oxygen-rich atmosphere (CO_2/O_2) and found that an increase in oxygen concentration promoted combustion. Bagheri et al. [11] explored the feasibility of municipal sludge as an energy source and found that the mixture of municipal sludge and straw had good combustion characteristics. In addition, he measured the phosphorus element in municipal sludge, confirming its certain recycling value. However, the composition of paper sludge was significantly different from municipal sludge and needed a different consideration. Thus, there is currently numerous studies on the properties of the direct combustion of paper sludge. The direct combustion of paper sludge needs to be investigated.

In addition, this paper also focuses on chemiluminescence, which is a phenomenon of light radiation accompanying the process of a chemical reaction. Chemiluminescence can provide useful information, including the state of combustion, such as the location of the reaction zone, the equivalence ratio, and the heat release rate. Chemiluminescence can also reflect the distribution of free radicals. CH* is an important free radical for measuring combustion reactions, and it has a characteristic chemiluminescence band at 431 nm. For instance, Ye et al. [12] characterised the ignition delay of pulverised coal fuel by eliminating the chemiluminescence information of visible light in the background. Simões et al. [13] utilised similar observation methods to extend the method of determining ignition delay to biomass fuels.

Our study focussed on the concept of using the sludge powder to form briquette fuel; the combustion characteristics of pure sludge was studies and its feasibility in combustion units, such as grate furnaces and fluidised beds, was examined. A flat flame burner was used as the heat source to achieve fast warming experimental conditions. The combustion of sludge briquettes (particles) was analysed and examined from several perspectives using optical observation techniques, narrow bandpass filters, and thermogravimetric systems. The optical timing diagram of a sludge particle on a burner was used to analyse the flame patterns, such as flame size, intensity and burn time. In addition, this study also analysed the combustion from a chemiluminescence perspective. The distribution diagram of CH* was used to study the apparent structure and ignition pattern of the sludge flame. The data on temperature changes and mass loss enabled the acquisition of the combustion rate and degree of burnout of sludge particles. The results of these experiments enabled the generalisation of the sludge particle burning process of under fast heating conditions, and suitable operating conditions for sludge burning in actual incineration treatment were obtained.

Fig. 1 Received paper sludge

Fig. 2 Paper sludge powder

Research method

Experimentals

Figures 1–3 depict the treatment procedure for paper sludge, including the received paper sludge, its powder and its particles. After being crushed, dried, and compressed, the paper sludge was formed into particles with a diameter of 0.5–0.6 cm under a pressure of 10 MPa. A single particle size was comparable to the biomass created and consumed in a circulating bed. Sludge particles weighed approximately 0.2816 g, had a volume of 0.2 cm^3 and had a density of 1.408 g/cm^3. The proximate analysis and ultimate analysis of paper sludge are displayed in Table 1.

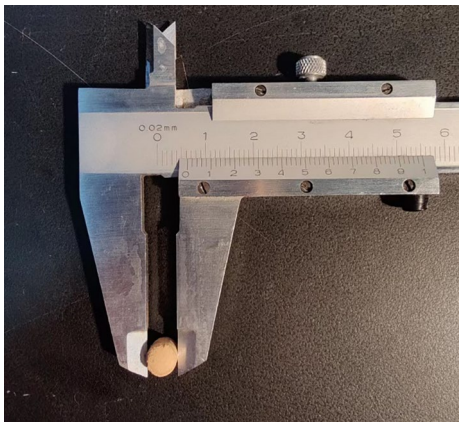

Fig. 3 Paper sludge particle

According to the test results, the moisture content of paper sludge is approximately 7.92%, the ash content is approximately 45.9%, the volatile content is approximately 39.22%, and the fixed carbon content is approximately 6.96%. Amongst the elements in paper sludge, carbon accounts for 24.32%, hydrogen accounts for 2.24%, oxygen accounts for 17.82%, and nitrogen and sulphur account for relatively low percentages of 0.86% and 0.36%, respectively. The ash content in the paper sludge mentioned earlier [3] is approximately 45%, which is similar to our result. Using Mendeleev's formula to calculate the low calorific value of paper sludge, the calculated low calorific value of paper sludge is approximately 7836.40 kJ/kg.

Solid waste typically has a modest calorific value that may self-sustain burning in boilers when it surpasses 3300 kJ/kg. The average calorific value of municipal solid waste (MSW) is approximately 5000 kJ/kg, whilst the calorific value of paper sludge is close to 8000 kJ/kg; this value is much higher than that of MSW. At present, there are power plants that use MSW as fuel for co-combustion with coal [14]. Paper sludge has a higher calorific value than MSW, and its effect as power plant fuel is better.

Experimental system and methods

The experimental system is shown in Fig. 4, with the measurement of temperature and mass loss on the left and the optical observation and measurement of CH* on the right. The combustion device of this experiment was a flat flame burner. Methane and air were mixed and flowed from below the burner to create a flat flame above the burner. The experimental material sludge was formed into particles and placed on a bracket. The end of the support bracket was positioned in the centre directly above the flat flame burner. When the burner produced a flat flame, the sludge particle at the end of the support bracket was ignited by the heat. At the same time, the base of the support bracket was placed on top of the electronic balance, which was zeroed before the particle was placed, and after, the data on the electronic balance display were sampled every 0.1 s using a data collector.

The surface of the particle came into contact with the hot end of the thermocouple. The thermocouple measured the temperature of the boundary layer on the surface of the particle. The cold end was connected to the computer via the port of the temperature control element. The temperature of the boundary layer on the surface of the particle was read out, and a temperature rise curve was obtained. At the same time, the burning state of the sludge particle was recorded

Table 1 Proximate analysis and ultimate analysis of the paper sludge powder

Sample	Proximate analysis w_{ad}/%				Ultimate analysis w_{ad}/%				
	M	A	V	FC	C	H	O	N	S
sludge	7.92	45.90	39.22	6.96	24.32	2.24	17.82	0.86	0.36

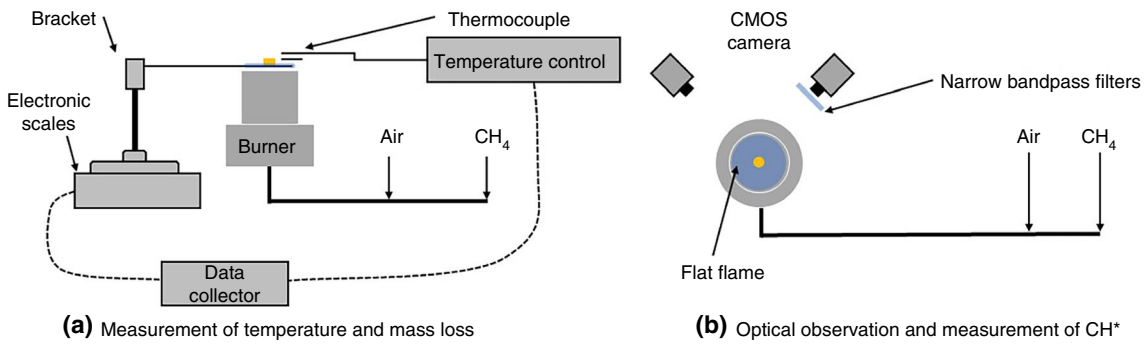

Fig. 4 Experimental system

using a CMOS camera, and the ignition and burning situation was determined according to the optical timing diagram.

A narrow bandpass filter at 430 nm was added in front of the camera lens to collect the optical signal in that band. The wavelength of CH* chemiluminescence was 430 nm, which enabled the speculation of the distribution of CH*. CH* is an important parameter indicating the state of combustion, and the presence of this radical means that the combustion entered its most intense phase. Its light emission is in the visible wavelength band, and therefore, the effect from natural light needs to be subtracted from the image. The experiment was conducted in a dark room to minimise the influence of natural light. Our assumption was that the luminescence at 430 nm generated by other factors in the combustion was negligible compared to the chemiluminescence from CH*. The images of CH* radical chemiluminescence were compared with the optical timing diagrams to enable analysis of the combustion process in the sludge particles.

By maintaining a constant methane flow rate and a flat flame and changing the air flow rate, different combustion atmospheres were generated. To minimise the methane flame influence on the sludge combustion and to use the flame only as a heat source, the sludge needed to produce a flame that was independent of the flat flame. The methane flow rate was adjusted to a low level of 5% of the flowmeter range of 3 L min^{-1} with an actual flow rate of 0.15 L min^{-1}. Next, the air flow was adjusted such that the methane flame could form a flat flame in a methane-air atmosphere. This paper used five operating conditions, and the specific information is shown in Table 2.

Analysis and discussion

Analysis of optical sludge combustion

The timing diagrams of the sludge compression combustion under different operating conditions are shown in Fig. 5a–e. From the figure, the sludge combustion was divided into two stages: the volatile combustion stage with an evident volatile flame and the coke combustion stage. The ignition time, combustion duration, flame limit height, and other information of the sludge were also observed in the figure. Below is the specific analysis.

From Fig. 5a, the flame began to appear at 20 s and disappeared at 62 s, indicating the end of volatile combustion; after, the sludge particle turned to coke combustion. The height of the volatile flame showed a trend of initially increasing and then decreasing, reaching its maximum at 7 cm at 42 s.

Figure 5b–e show the combustion optical time series diagrams of operating conditions 2 to 5. Due to a similar trend between each time series diagram, only the differences were provided. The ignition time, extinguishment time, highest flame, and volatile combustion time of the combustion under various operating conditions are listed in Table 3.

The combustion of sludge particles was solid fuel combustion, and a heterogeneous reaction occurred at the contact surface between the fuel and gas. The material flow generated in the normal direction of the phase interface became the Stefan flow [15]. The Stefan flow had almost no effect on the surface temperature and combustion rate of sludge particles; however, it could cause fuel vapour to flow outwards. The shape of the volatile flame was affected by this.

The combustion was divided into two stages: volatile combustion in the early stage and coke combustion in the later stage. Volatile combustion was accompanied by a significant volatile flame, with flame height initially increasing and then decreasing and temperature sharply increasing. Through comparison, with changes in the operating conditions, there was no significant change in the timing of sludge particle ignition. Under different operating conditions, sludge particles generated observable volatile flames starting at approximately 16 s.

The height and brightness of the flame reflected the Stefan flow intensity on the surface of sludge particles, which could be used to compare the intensity of combustion. The most vigorous stage of volatile flame combustion occurred at approximately 40 s–45 s. At this point, the length and brightness of the flames reached their highest values. Under operating condition 1, when the O_2 content was 4%, the maximum flame was approximately 7 cm. Under operating conditions 3 and 4, the flame height significantly increased, reaching a maximum of approximately 11 cm. Under the operating condition 5, the maximum flame height was only

Table 2 Different combustion conditions on a flat flame burner

Operating condition	CH_4/L min^{-1}	O_2/L min^{-1}	N_2/L min^{-1}	Temperature/℃	O_2/%
1	0.15	0.378	1.422	1122	4.00
2	0.15	0.441	1.659	1109	6.27
3	0.15	0.504	1.896	1094	8.00
4	0.15	0.567	2.133	1091	9.37
5	0.15	0.630	2.370	1077	10.48

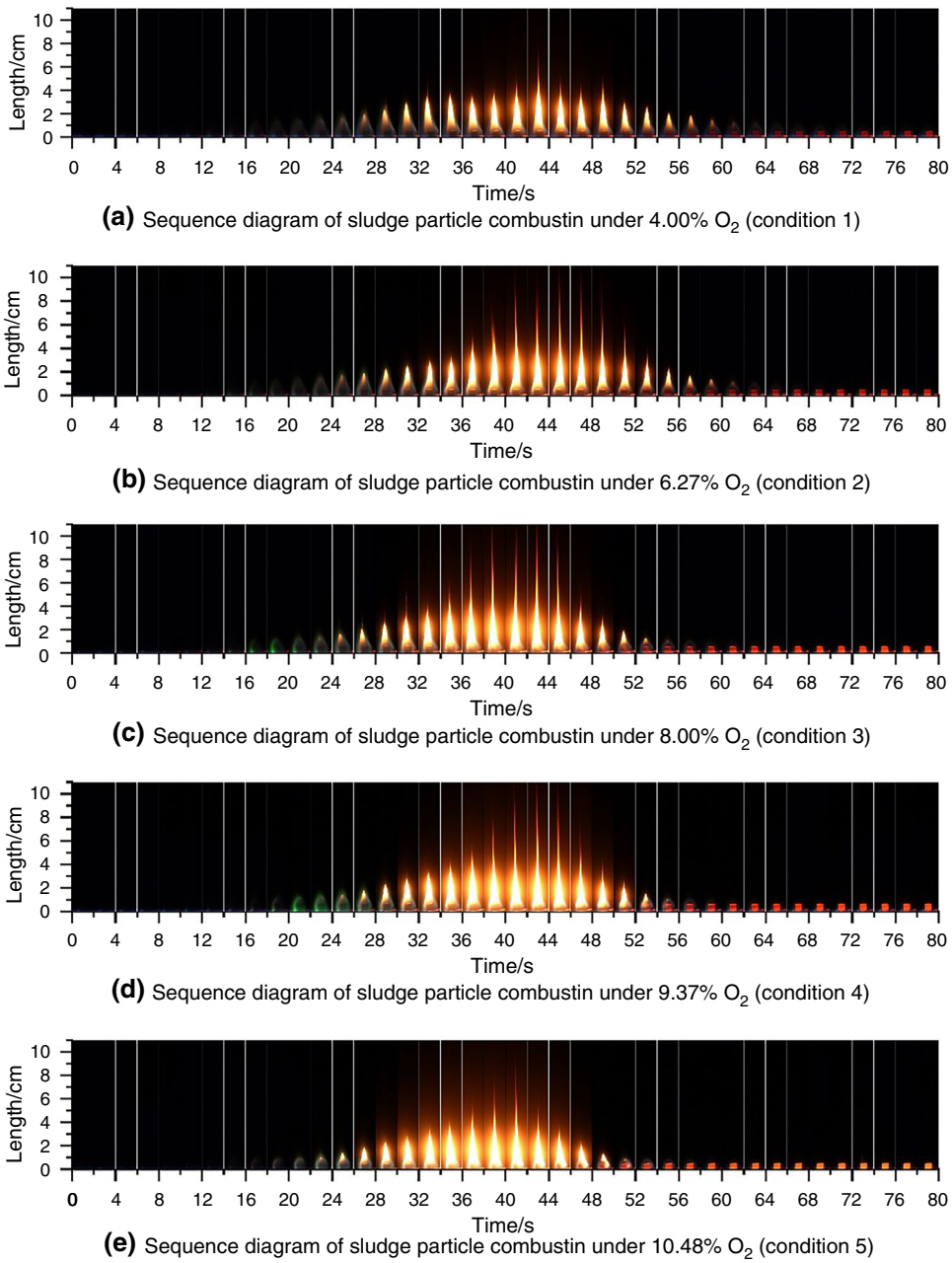

Fig. 5 Optical time series diagram of the sludge combustion

Table 3 Comparison of the optical time series diagram parameters of paper sludge

Operating condition	Ignition time/s	Extinguishment time/s	Highest flame/cm	Volatile combustion time/s
1	16	64	7	48
2	16	62	10	46
3	16	58	11	42
4	16	56	11	40
5	16	52	10	36

approximately 10 cm. However, at this time, the width and brightness of the flame significantly increased, which was caused by the more intense Stefan flow. This was reflected in the more intense combustion of the sludge particles.

The flame of sludge particles began to disappear at 52 s to 64 s. A higher oxygen content correlated to a faster consumption of the volatile matter and an earlier disappearance of the flame. When the oxygen concentration was 4.00%, the combustion duration of volatile matter was 48 s, and when the concentration rose to 10.48%, the combustion duration of volatile matter was 36 s. The gradual end of volatile combustion represented the sludge

particle entering the coke combustion state. Coke combustion dominated after the completion of volatile combustion. As the oxygen content increased, the brightness of coke combustion also increased, changing from dark red to bright yellow. Due to the formation of a layer of ash shell on the surface of the sludge tablet after combustion, which hindered the reaction between oxygen and the internal environment, the combustion of coke was relatively long, approximately 10 min.

Analysis of chemiluminescence

Figure 6a–e shows the flame image filtered by a 430 nm narrow bandpass filter. By greying out the original image and inverting it, more evident chemiluminescence and carbon smoke radiation images were obtained. A dashed line was used to separate the enveloping region below and the wake region above, with carbon smoke radiation dominating above the line and chemiluminescence of CH * below the line. Below is a brief analysis.

Figure 6a shows the filtered flame image at an oxygen concentration of 4.00%. From the graph, starting from 22 s,

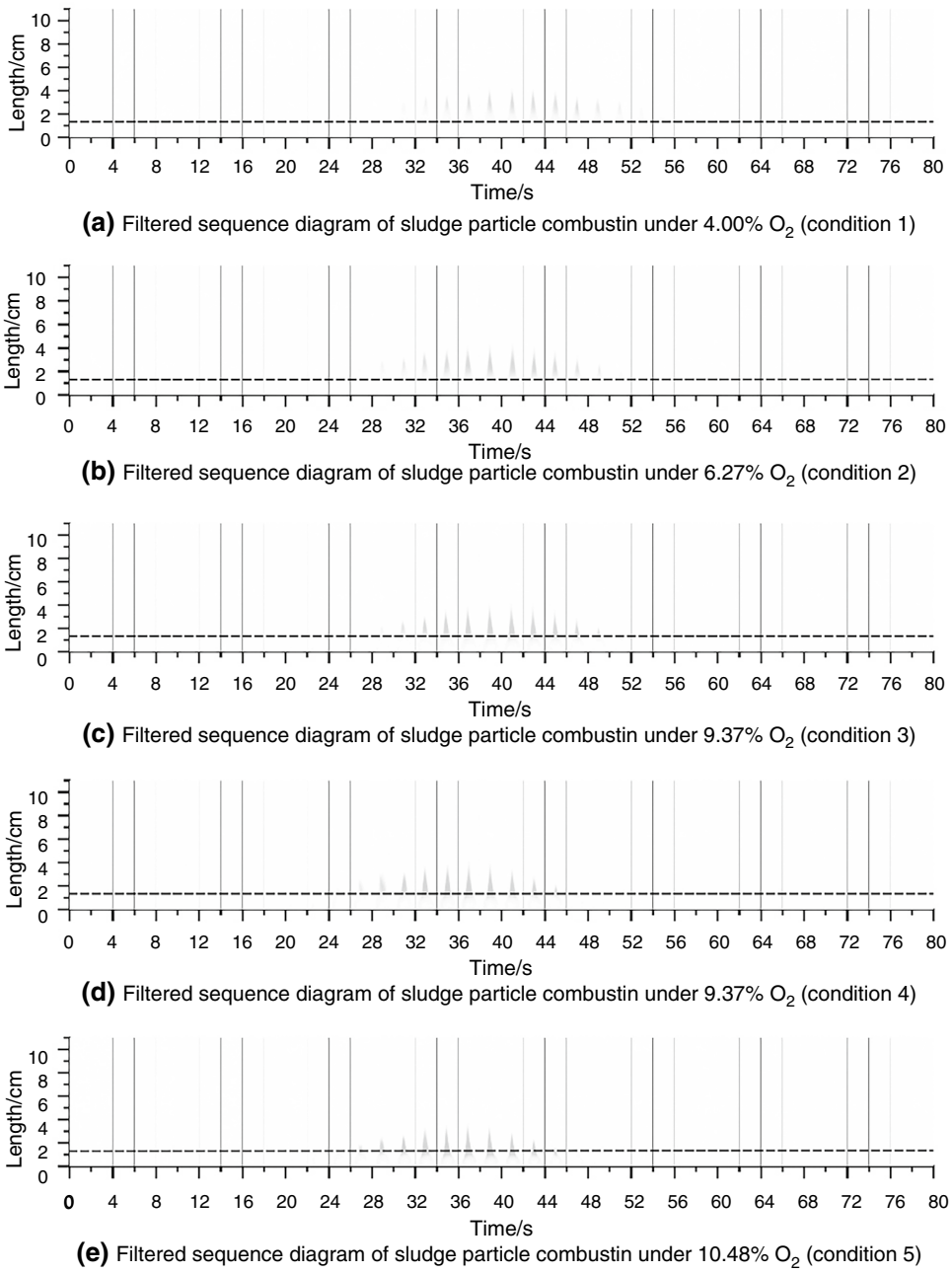

Fig. 6 Filtered optical time series diagram of the sludge combustion

weak CH* chemiluminescence was observed. Afterwards, the chemiluminescence intensity of CH* initially increased and then decreased and finally disappeared at approximately 54 s.

Figure 6b–e shows the flame-filtered images at oxygen volume concentrations ranging from 6.27 to 10.48%. The overall trend was similar to Fig. 6a; the filtered flame shape was similar and the brightness also showed a trend of initially increasing and then decreasing. The changes in size, such as the flame height, of the filtered flame were not as significant as the height changes in the original flame image. The CH* free radical was only distributed at a fixed position in the volatile flame and concentrated in the inner flame, and the closer CH* was to the centre of the flame correlated to a higher concentration. From this, CH* free radicals were generated near the surface of the sludge tablet and were only intermediate products of the combustion process. They were oxidised to CO_2 and H_2O outside the flame.

As the operating conditions changed and the oxygen content in the atmosphere increased, the timing of the filtered flame image also changed; this result was different from the original flame image of the sludge particle. Under operating condition 1, when the oxygen content was 4%, the filtered flame image appeared in 28 s–54 s. However, under operating condition 5, when the oxygen content was 10.48%, the image appeared in 22 s–28 s. The timing of the occurrence of the CH* free radicals was more sensitive to oxygen concentration, which could affect the severity of combustion; a higher oxygen content correlated to a more intense combustion, an earlier occurrence of the CH* free radicals, and a faster depletion of the free radicals. In addition, as the oxygen concentration increased, the amount of CH* radicals consumed per unit time also increased. This result could be observed from the filtered colour brightness of the flame, which indicated that the chemiluminescence became more intense.

The filtered flame disappeared before the original flame image, indicating that CH* radicals were no longer generated during the later stage of volatile combustion. This result was potentially caused by the rapid consumption of hydrogen in volatile matter. In the combustion stage of the coke after the volatile matter was burned out, H was already completely depleted, and at this time, the CH* free radical was not observed at all.

Analysis of temperature and mass loss

Figure 7 shows the temperature rise curves of sludge particles under different operating conditions. From the figure, the operating conditions 1–3 were observed as a group, and their curves were similar to the first-order response curve. Operating conditions 4–5 were observed as another group, and their curves were similar to the second-order

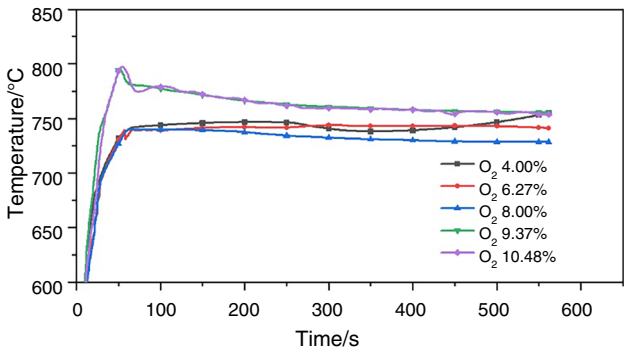

Fig. 7 Temperature rise curve of boundary layer on the surface of the sludge particles

response curve. The heating curves of these two groups were relatively similar. In the early stage of volatile combustion, from 0 to 25 s, all operating conditions were rapidly heated, and the heating curves were consistent. At this stage, there was no significant combustion of the sludge particles. The moisture in the tablet rapidly evaporated, and the chemical bonds of cellulose, hemicellulose and lignin began to break, releasing volatile matter. When heated, cellulose and hemicellulose produced liquid tar [16], promoting ignition.

At approximately 25 s–50 s, the slope of the heating curve gradually decreased, and differentiation began to occur between the curves. The slopes of operating conditions 4 and 5 were higher than those of the other three conditions, resulting in faster heating. At this stage, the combustion of sludge particles was in diffusion combustion, and the heating rate was related to the oxygen content in the atmosphere. A higher oxygen content corresponded to a faster temperature increase and higher maximum temperature. A higher oxygen content could cause more oxidants to diffuse near the particle surface per unit time, resulting in more intense combustion. The significant heating stage ended at approximately 50 s, and the temperature reached its highest value. Compared with the optical timing chart, the combustion of volatile matter was approaching the end, and the particles were about to turn into coke for combustion. The sludge particles always maintained a significant temperature rise during the combustion process of volatile matter.

The heating curve of sludge particles was mainly divided into three stages. During the rapid heating stage, the temperature rapidly increased under various operating conditions, and the heating curve was almost consistent. In the stage where the heating rate decreased, the heating rate and maximum temperature increased with increasing oxygen content. In the stable stage, the sludge particles entered a stable coke combustion state, and the temperature tended to be constant, slowly changing with time.

Figure 8 shows a comparison of the mass loss of sludge particles under different operating conditions. Below is a brief analysis of the mass.

The trends of the mass loss curves under different operating conditions were similar. To compare the differences in detail, the parameters are listed in Table 4.

The maximum temperatures of operating conditions 1–3 occurred at approximately 50 s, ranging from 740 to 750 ℃. The maximum temperatures of operating conditions 4–5 were approximately 800 ℃, and a temperature decrease process was observed after the highest temperature occurred. The final temperature of several curves gradually stabilised. This occurred because after the volatile matter had been burned out, the sludge entered the coke combustion stage. In this stage, the oxygen in the gas only reacted with the coke on the surface of the compression particle, with a lower reaction rate and always abundant oxygen. Therefore, the combustion intensity in this stage was relatively high and was less affected by the oxygen content.

Referring to the heating curve, the mass loss curve could also be roughly divided into three stages. The first stage started from the beginning of heating to the early stage of volatile combustion; this started at 0 s and ended in 25 s to 30 s. All operating conditions experienced rapid mass loss, and the mass loss rate gradually increased. At this stage, the sludge particles released moisture and volatile matter, which was ignited near the particle and rapidly increased. The highest mass loss rate occurred at the end of the first stage.

According to proximate analysis, the final residual mass of the paper sludge after combustion should be approximately 56%, which was the sum of ash and fixed carbon. However, the mass loss curve showed that the mass of the paper sludge particles under operating condition 1 was ultimately stable at approximately 75%, and the mass under operating conditions 2–5 was ultimately stable at approximately 72%. These results indicated that the volatile matter combustion of sludge particles was also incomplete.

Table 4 Comparison of the temperature and mass loss parameters

Operating condition	O_2 / %	Max temperature / ℃	Residual mass / %	Max mass loss rate / % s^{-1}
1	4.00	746.73	75.06	0.54
2	6.27	743.39	72.33	0.57
3	8.00	741.52	72.16	0.71
4	9.37	796.14	72.05	0.79
5	10.48	797.04	72.02	0.86

The limitation of the oxygen content led to a phenomenon of "snatching air" on the surface of particles [17], which could cause local hypoxia on the surface of sludge particles, thereby inhibiting the release of volatile substances.

Thermogravimetric analysis

Thermogravimetric analysis is applied in many fields. The thermal stability, pyrolysis status, intermediate products and pyrolysis products of the sample materials can be determined by analysing the thermogravimetric curve. In addition, under rapid heating conditions, the various volatile components and moisture in the paper sludge began to be lost at almost the same time, resulting in only one peak in its mass loss curve. To gain a more detailed understanding of the chemical reaction parameters during the pyrolysis and combustion process of paper sludge, conventional thermogravimetric experiments were also conducted on the samples.

The mass of the paper sludge particles in this experiment remained stable at approximately 72% after combustion, which was significantly different from 56%. Therefore, it was necessary to investigate the residual volatile content in the burnt sludge particles. A thermogravimetric experiment was conducted on the sludge and sludge ash after the combustion experiment. Figure 9 shows the results of the thermogravimetric experiment, which are briefly analysed below.

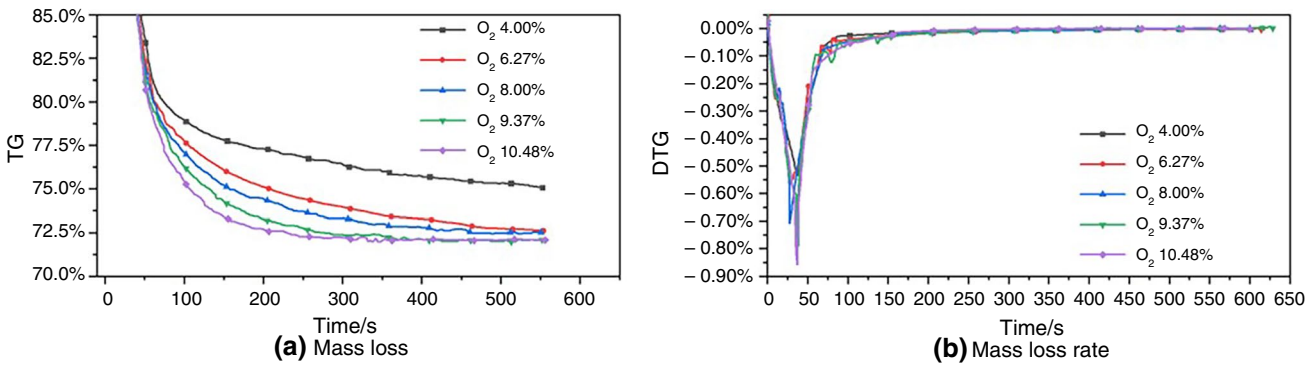

Fig. 8 Mass loss curve of the sludge particles

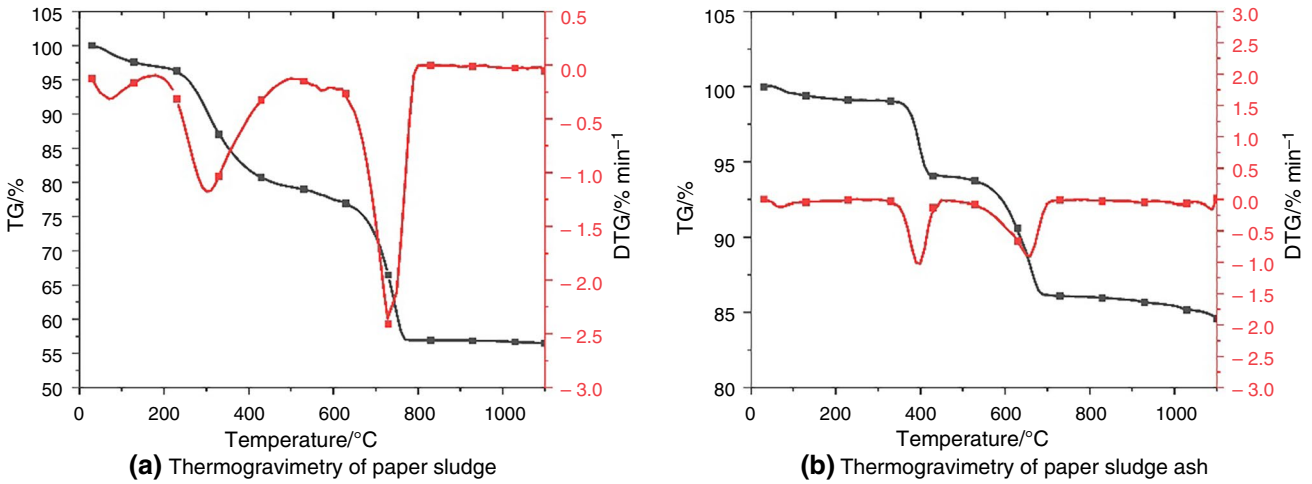

Fig. 9 Thermogravimetric analysis

Our thermogravimetric analysis used a German Netzsch STA 2500 thermogravimetric analyser to conduct thermogravimetric experiments at a heating rate of 5 °C min^{-1}. The experimental materials were the paper sludge and paper sludge ash. The specific heating process started at room temperature, and the temperature was increased at a rate of 5 °C min^{-1} to 1100 ℃. The thermogravimetric curve of paper sludge is shown in Fig. 9a, whilst the thermogravimetric curve of paper sludge ash is shown in Fig. 9b.

According to Fig. 9a, there were three mass loss peaks. The first mass loss peak appeared at 79.5 ℃, at which point the mass loss rate of the sludge was − 0.31% min^{-1}. This mass loss peak was mainly caused by water evaporation. After, when the temperature rose to 304.2 ℃, the second mass loss peak appeared, and the mass loss rate of the sludge was − 1.18% min^{-1}. At this time, the main mass loss of the sludge was the release of the volatile matter. After these two peaks, the paper sludge lost approximately 21% of its mass. According to proximate analysis, the moisture content in the air dry basis of paper sludge was 7.92%, and the volatile content was 39.22%. Therefore, at this time, the moisture of paper sludge was completely removed, and the volatile content was partially lost. The third mass loss peak appeared at 735.7 ℃, at which time the mass loss rate of paper sludge was − 2.49% min^{-1}, and the release of volatile matter dominated the mass loss at this time. After these three peaks, when the temperature was above 763.3 ℃, the mass loss rate of paper sludge approached zero and finally stabilised at 56.53%. According to proximate analysis, the ash content of papermaking sludge was 45.9%, the fixed carbon content was 6.96%, and their sum was 52.86%; this value was similar to the final quality residue of the paper sludge. The thermogravimetric data of paper sludge indicated that fixed carbon had difficulty participating in combustion.

From Fig. 9b, two mass loss peaks were observed in the thermogravimetric curve of paper sludge ash after combustion. The first mass loss peak appeared at 395.3 ℃, with a mass loss rate of − 1.05% min^{-1}, which was similar to the second mass loss peak of the original sludge in Fig. 9a. The second mass loss peak appeared at 656.1 ℃, with a mass loss rate of − 0.92% min^{-1}. After these peaks, the remaining mass accounted for 84.58% of the original mass. No mass loss peak was observed for the water release in the thermogravimetric curve of sludge ash, and both mass loss peaks were caused by volatile matter loss. This result also confirmed the previous deduction that the dense ash shell formed on the surface of sludge particles and prevented their internal combustion, and a large amount of volatile matter was not released, which accounted for 35.48% of the total volatile matter. Therefore, in the process of pressing sludge, the formation of porous particles could be considered to increase the contact area between sludge and air to facilitate more complete combustion.

Conclusions

Exploring harmless and resourceful treatment methods for paper sludge has certain economic and environmental significance. The dynamic detection of temperature and quality is of great significance for the quantitative analysis of the combustion process, which enables the optimisation and adjustment of combustion parameters to obtain the optimal combustion conditions. Below is a summary of the conclusions of this article.

Increasing the oxygen content did not have a significant impact on the ignition time of sludge particles, but it could significantly increase the combustion rate. As the oxygen content increased, the flame brightness significantly

improved, and the burn out time of the volatile matter improved. The chemiluminescence of CH* occurred in the most intense stage of sludge particle volatile combustion, and a filtered flame appeared in a certain area inside the volatile flame and disappeared earlier than the volatile flame. As the oxygen content increased, CH* was depleted earlier, indicating that H in the sludge particles was depleted earlier.

There were significant differences in the heating curves and mass loss curves of the paper sludge particles under different operating conditions. When the oxygen content was low (operating conditions 1–3), the heating curves were similar to the first-order response curve, with a monotonic increase in temperature. When the oxygen content was slightly higher (operating conditions 4–5), the heating curves were similar to the second-order response curve, with small fluctuations. A higher oxygen content led to faster heating. In addition, the maximum temperature and heating rate also increased with increasing oxygen content.

The effect of oxygen content on the degree of burnout was observed from the mass loss curves. The lower oxygen concentration could not fully penetrate the ash shell on the surface of the particles and react with the internal sludge, which led to a lower degree of burnout. According to the results of the thermogravimetric experiment, the internal volatile matter did not fully participate in the reaction during the combustion of sludge particles. A porous structure could help to improve the degree of burnout by increasing the specific surface area, which could be a feasible solution to promote combustion.

Acknowledgements Key Project of the National Natural Science Foundation of China: The Migration behaviour of Alkali Metals in High Alkali Solid Fuel Combustion and Its Microregulation on Pollutant Generation

References

1. 2020 Annual Report of China's Paper Industry. China Paper Newsletters, 2021; no 05, pp 6–16
2. Kaur R, Tyagi RD, Zhang X. Review on pulp and paper activated sludge pretreatment, inhibitory effects and detoxification strategies for biovalorization. Environ Res. 2020;182:109094. https://doi.org/10.1016/j.envres.2019.109094.
3. Mao R, Shao J, Wang G, et al. Thermal behaviour and kinetics analysis of co-combustion of petroleum coke and paper sludge-derived hydrochar. Waste Manag. 2022;153:405–14.
4. Saastamoinen J, Aho M, Moilanen A, et al. Burnout of pulverised biomass particles in large scale boiler—single particle model approach. Biomass Bioenerg. 2010;34(5):728–36.
5. Bridgeman TG, Jones JM, Shield I, et al. Torrefaction of reed canary grass, wheat straw and willow to enhance solid fuel qualities and combustion properties. Fuel. 2008;87(6):844–56.
6. Kihedu J. Torrefaction and combustion of Ligno-cellulosic biomass. Energy Procedia. 2015;75:162–7.
7. Bach Q, Tran K, Skreiberg Ø, et al. Effects of wet torrefaction on pyrolysis of woody biomass fuels. Energy. 2015;88:443–56.
8. Wang S, Wen Y, Hammarström H, et al. Pyrolysis behaviour, kinetics and thermodynamic data of hydrothermal carbonization–Treated pulp and paper mill sludge. Renew Energy. 2021;177:1282–92.
9. Zhang Z, Sun G, Duan L. Combustion characteristic and pollutants emission behaviour during co-combustion of coal and municipal sewage sludge. Clean Coal Technol. 2022;28(03):118–29.
10. Bi S. Research on combustion characteristics of sludge mixed with coal and emission characteristics of conventional pollutants under O_2/CO_2 atmosphere. Shandong University, (2018)
11. Bagheri M, Öhman M, Wetterlund E. Techno-economic analysis of scenarios on energy and phosphorus recovery from mono- and co-combustion of municipal sewage sludge. Sustainability. 2022;14(5):2603–28.
12. Yuan Y, Li S, Li G, et al. The transition of heterogeneous–homogeneous ignitions of dispersed coal particle streams. Combust Flame. 2014;161(9):2458–68.
13. Simões G, Magalhães D, Rabaçal M, et al. Effect of gas temperature and oxygen concentration on single particle ignition behaviour of biomass fuels. Proc Combust Inst. 2017;36(2):2235–42.
14. Jamasb T, Nepal R. Hot issue and burning options in waste management: a social cost benefit analysis of waste-to-energy in the UK. Resour Conserv Recycl. 2010;54(12):1341–52.
15. Hurt R H, Mitchell R E. On the combustion kinetics of heterogeneous char particle populations. In: 24th International symposium on combustion, 1991; vol 24, no 1, pp 1233–1241
16. Senneca O, Cerciello F, Russo C, et al. Thermal treatment of lignin, cellulose and hemicellulose in nitrogen and carbon dioxide. Fuel. 2020;271:117656.
17. Liu H, Okazaki K. Simultaneous easy CO_2 recovery and drastic reduction of SOx and NOx in O_2/CO_2 coal combustion with heat recirculation. Fuel. 2003;82(11):1427–36.